*Progress In Electromagnetics Research B, Vol. 38, 225–239, 2012*

# CHARACTERIZATION OF OPEN CELL SIC FOAM MATERIAL

**I. Zivkovic*** **and A. Murk**

Institute of Applied Physics, University of Bern, Siedlerstrasse 5, Bern 3012, Switzerland

**Abstract**—This paper presents characterization and modeling of microwave characteristics of SiC foam material. Transmission and reflection measurements are performed in X, K and Ka band for the samples of two different pore sizes and three different thicknesses. Effective and frequency dependent dielectric permittivity is extracted for 50PPI 10 mm sample, while for the other samples it was not possible because of density gradient in the samples. By calculation of Mie scattering efficiencies approximate magnitude of dominant loss mechanism (scattering or absorption) at certain frequencies is predicted.

## 1. INTRODUCTION

Different materials and structures can be used as absorbers of microwave energy [1–3]. One possible candidate as microwave absorber is Silicon Carbide foam. Silicon Carbide (SiC) foam is complex material. It is lightweight and with very good thermal conductivity (can survive very high temperatures). There are wide varieties of SiC foam applications such as: high temperature applications (filters, heat exchanges, heat shielding, etc.), gas diffusers for semiconductor manufacturing, porous electrodes, absorbers of electromagnetic radiation [4–6] etc..

We are interested in using SiC foam as absorber of electromagnetic energy at microwave frequencies. In the literature [7–10] there is some information about SiC foams but usually limited only to the X frequency band. Measurements that we performed are at X, K and Ka frequency bands. There are also attempts to make a model and perform

*Received 15 December 2011, Accepted 17 January 2012, Scheduled 22 January 2012*

* Corresponding author: Irena Zivkovic (irena.zivkovic@iap.unibe.ch).

numerical simulations of SiC foam material [9, 10]. Since geometry of the foam is complex, numerical simulations do not represent real situation. Because of that, we must rely on measurements and draw conclusions from comparison of measurements of the samples with different foam characteristics (different number of pores per inch) and different sample thicknesses.

We performed transmission as well as reflection measurements with metal on the back side of samples. Samples that are examined are of different thicknesses and different geometrical characteristics. From the amplitude and phase of the transmission measurements Debye model of the complex and frequency dependent permittivity can be calculated, but only for materials that are isotropic and homogeneous with respect to used $\lambda$ [14]. We extracted Debye model for 50PPI 10 mm thick sample.

## 2. SIC FOAM MATERIAL CHARACTERISTICS

SiC is a compound of silicon (Si) and carbon (C). If grains of SiC are bonded together by sintering process, very hard ceramic is formed. Pure SiC is dielectric material with very low loss. Eq. (1) represents frequency dependent dielectric permittivity of pure SiC expressed with Debye relaxation formula [11]. Electrical properties of SiC become different by doping with different elements [7, 8]. Eq. (2) represents frequency dependent dielectric permittivity of doped SiC (SiC-B, CERASIC-B manufactured by Toshiba Ceramics Co. Ltd.) [16]. Figure 1 gives graphical representation of Eqs. (1) and (2). Pure SiC material has very low relaxation frequency (0.013 GHz) and because of

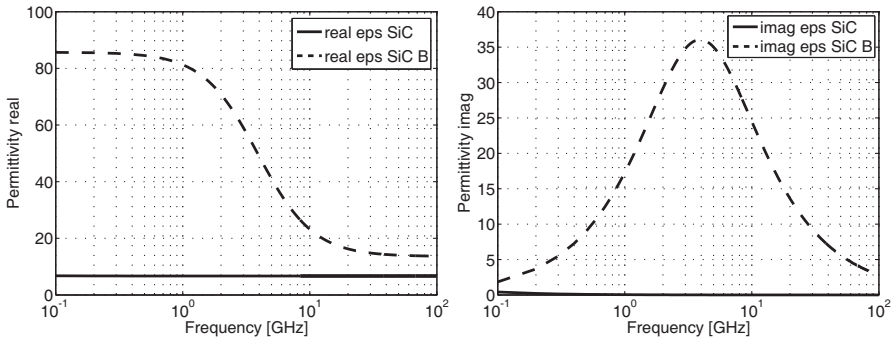


**Figure 1.** Plot of real and imaginary parts of pure SiC and SiC-B. Plots are made from Eqs. (1) and (2).

that at microwave frequencies it has constant real and imaginary parts of permittivity. Imaginary part of permittivity very fast approaches zero. In SiC-B material dielectric losses are increased (imaginary part of permittivity is larger than zero what is seen in Figure 1). Density of bulk SiC material is 3.21 $\frac{\text{g}}{\text{cm}^3}$ [15] and SiC-B has the same density [16].

$$\varepsilon_{SiC}(f) = 6.7 + \frac{3.3}{1 + \frac{jf}{0.013}} \tag{1}$$

$$\varepsilon_{SiC\text{-}B}(f) = 13.6 + \frac{72.1}{1 + \frac{jf}{3.92}} \tag{2}$$

$f$ is frequency in GHz.

Synthetic SiC can be found in many different forms and one of them is complex foam structure. Ideally, absorbing material should be with very low dielectric constant (in order to have better match with air which gives smaller reflection) and high loss (which can be increased by adding conductive particles). By foaming of material we increase porosity and effective dielectric constant decreases because of air which implies decreasing of reflection parameter. One characteristic of SiC foam material is volume fraction density. Volume fraction density represents percentage of bulk material contained in the foam. Another characteristic of SiC foam samples is number of pores per inch (PPI). Pore size depends on PPI number. Figure 2 shows a close up look at the unit cell of one kind of SiC foam material.

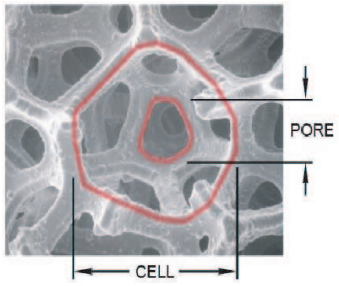


**Figure 2.** Closer look at the unit cell of SiC foam (www.ergaerospace.com).

Samples that we examined were provided by RUAG Technology, Switzerland. The base material is 'Cerasic CU' from Drache Umwelttechnik, Germany and normally is used as a filter for metal casting. We do not have any information about characteristics of bulk material from which samples are made.

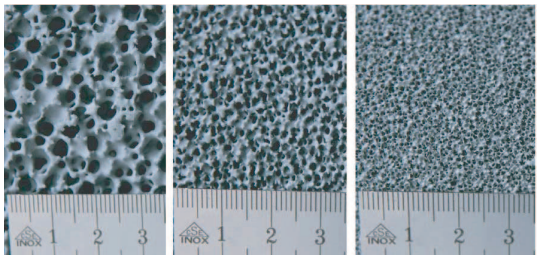

**Figure 3.** Photograph of three SiC foam samples with different pore sizes: 10PPI, 30PPI and 50PPI.

**Table 1.** Sample parameters.

| Sample | Dimension [mm] | Density $[\frac{g}{cm^3}]$ | Volume fraction |
|---|---|---|---|
| 10PPI | $395 \times 395 \times 11.2$ | 0.518 | 0.161 |
| 10PPI | $395 \times 395 \times 17.3$ | 0.577 | 0.180 |
| 10PPI | $395 \times 195 \times 29.0$ | 0.551 | 0.172 |
| 50PPI | $398 \times 398 \times 10.0$ | 0.557 | 0.174 |
| 50PPI | $399 \times 398 \times 18.2$ | 0.521 | 0.162 |
| 50PPI | $395 \times 394 \times 28.5$ | 0.490 | 0.153 |

Figure 3 represents SiC samples with different pore sizes which we have used for our measurements. There is a difference between structure presented in Figure 2 and material that we used. Our material is more 'closed' which means that it contains smaller number of open pores, rather they are full with material. Also, by visual inspection it is noted that there is density gradient in material which affects measurements and also has influence on material density. In the Table 1, some parameters of the samples that we examined are presented. From the Table 1 we see that materials with the same number of PPI and of different thicknesses have different densities. Cylindrical connections that form pores are ligaments. Ligaments can have the same cross section size for different number of PPI or different size of cross section for different PPI. If ligaments are of the same cross section for different PPI, then by increasing pore size (smaller PPI) volume fraction decreases. Materials that we examined have volume fraction 16 to 18 percents independently of the pore size, which means for the bigger pores (smaller PPI number) ligaments cross section is bigger.

## 3. MEASUREMENT RESULTS

### 3.1. Transmission Measurements

We performed transmission and reflection measurements on the samples SiC 10PPI and SiC 50PPI in three different thicknesses. Free space transmission measurements were performed in X, K and Ka bands with horn antennas that were designed for these bands. In X and K band measurements were obtained with HP 8510C Vector Network Analyzer (VNA) while in Ka band with an Abmm Vector Network Analyzer (Abmm VNA). For transmission measurements horn antennas are aligned and SiC foam sample is placed on the aperture of one of the antennas. Calibration for transmission measurements is $S_{21}$ measurement without sample between transmitting and receiving antenna. Figure 4 represents transmission measurements for 10PPI and 50PPI samples. In Figure 4 in the left graph is visible that measurement in Ka band becomes very noisy because dynamic range of the instrument is reached. The measurements are also repeated in W band, but because of the high losses no useful results were obtained.

### 3.2. Reflection Measurements

If we want to use SiC foam as electromagnetic wave absorbing material then reflection coefficient with metal backing (metal plate on the back side of sample) is of interest for us because it is close to the real situation. On the same samples that we performed transmission, we performed also reflection measurements with metal backing. We placed material samples with metal backing at the aperture of the antenna.

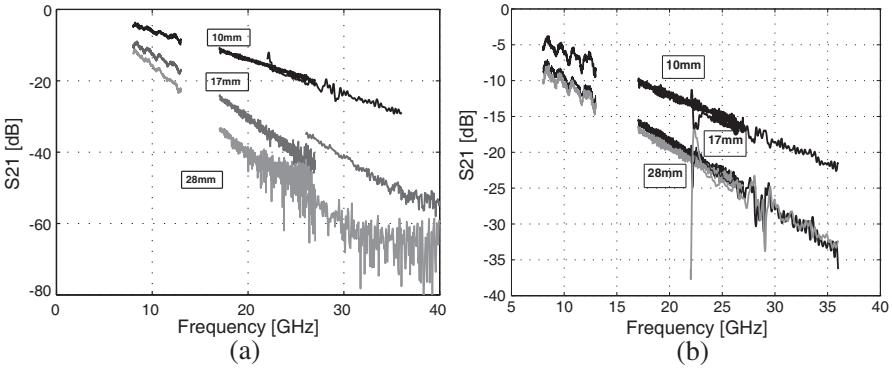


**Figure 4.** Measured transmission coefficient of 10PPI samples (a) and 50PPI (b). Examined samples are of three different thicknesses.

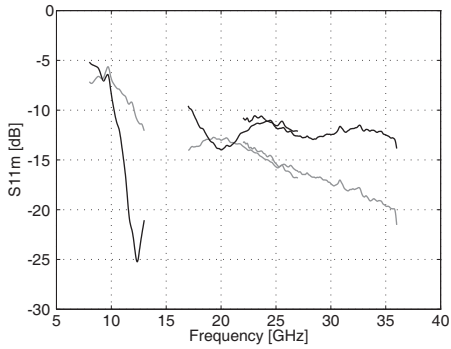


**Figure 5.** Measured reflection coefficient of 10PPI (gray line) and 50PPI (black line) 10 mm thick samples with metal backing.

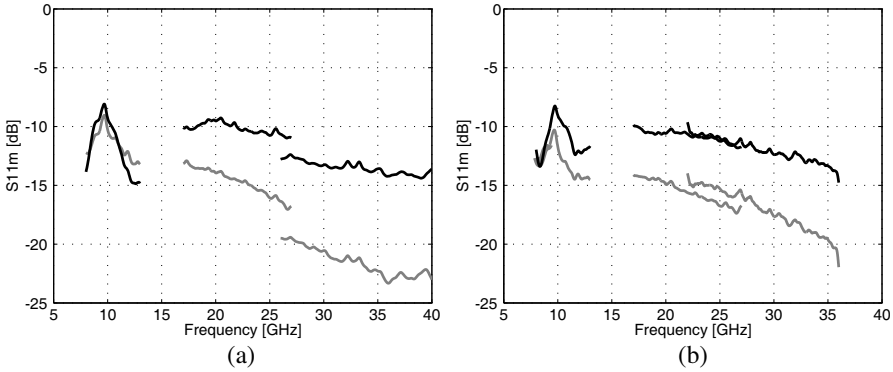


**Figure 6.** Measured reflection coefficient of 10PPI (gray line) and 50PPI (black line) 17 mm (a) and 28 mm (b) thick samples with metal backing.

Antenna is connected to the VNA through directional coupler. For calibration purposes we measure the reference signal (metal plate is on the aperture of the antenna, 100% reflection) and signal when the antenna is pointed on low reflectivity pyramidal foam absorber (to calibrate directivity).

Reflection measurements are performed in X and K band (on VNA) and in Ka (on Abmm VNA), Figures 5 and 6. Small inconsistency between measurements in X and K band on one and Ka band on the other side can be because we used different instruments for measurements in mentioned bands or because of density gradient in samples which cause different measurement results depending on which side of the sample is directed towards the antenna.

## 4. DISCUSSION ABOUT BULK MATERIAL OF EXAMINED SAMPLES

Since we do not have any information about material from which foam samples that we examined are made, we made some assumptions based on measurements and simulations. The first assumption is that bulk material is pure dielectric ($\mu = 1$). The second assumption is related to conductivity of bulk material. If pure SiC material is used (which permittivity is presented by Eq. (1)), because it is low loss and non conductive, according to simulations in [9, 10], reflection would be very high (close to 0 dB). From reflection measurements of our samples we can conclude that our material is conductive. In [17–19] summary of measurement techniques and techniques for permittivity extraction are presented. We fitted transmission measurement (both amplitude and phase) and from the fit permittivity model of the material (if material is homogeneous and isotropic) can be extracted. Extracted Debye model for permittivity of 50PPI 10 mm material sample (Eq. (3)) shows agreement between measured and simulated $S_{21}$, $S_{11}$ and $S_{11_m}$ (reflection with metal backing). Figures 7 and 8 represent measured and simulated scattering parameters. The agreement is better for the transmission data since it was used for the fitting. The slightly lower $S_{11}$ and $S_{11_m}$ results could indicate a difference from the assumed homogeneous sample and single pole Debye model. Fitted data is not consistent with 17 mm and 28 mm thick 50PPI samples. One possible explanation is different density of the samples which is obvious in Table 1.

$$\varepsilon(f) = 2.3 + \frac{2.426}{1 + \frac{jf}{17.74}} \tag{3}$$

$f$ is frequency in GHz.

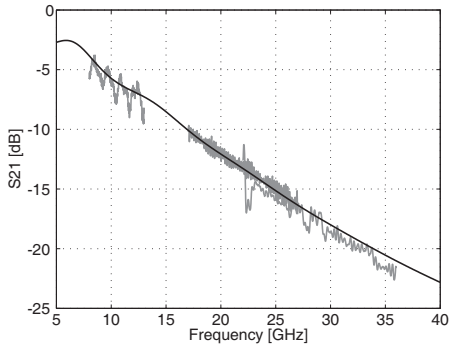


**Figure 7.** Measured transmission coefficient (gray line) of 50PPI 10 mm thick sample. Black line represents fitted Debye model.

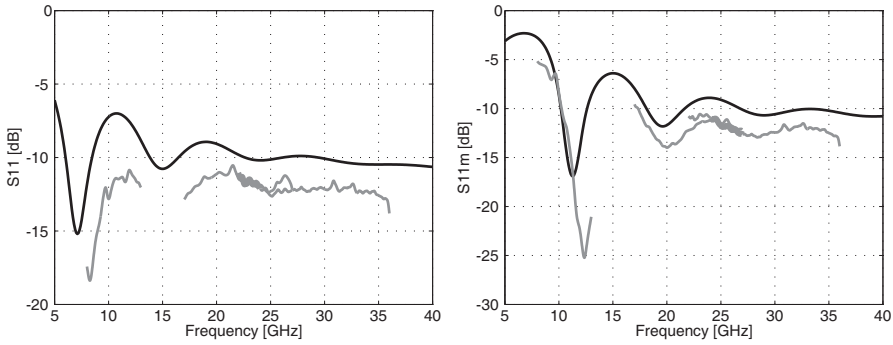


**Figure 8.** Measured reflection coefficients (gray lines) of 50PPI 10 mm thick sample without (left graph) and with (right graph) metal backing. Black lines represent reflection coefficients (for samples with and without metal backing) calculated from extracted Debye model.

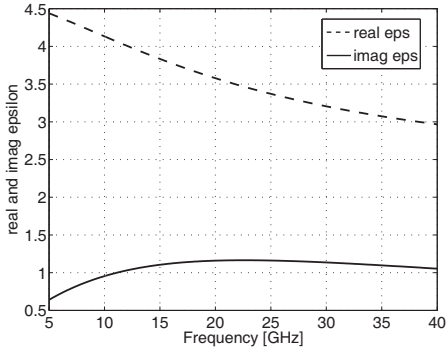


**Figure 9.** Real and imaginary part of extracted frequency dependent permittivity of 50PPI 10 mm SiC foam sample. This is graphical representation of Eq. (3).

We can conclude that at this frequency range (X to Ka band) optical property of 50PPI 10 mm thick sample can be described by a Debye model given by Eq. (3). Figure 9 represents real and imaginary parts of permittivity plotted from Eq. (3).

Permittivity of the solid material must be higher than effective permittivity of the 50PPI 10 mm thick sample (according to Maxwell Garnett mixing formula [14]). From extracted Debye model we can conclude that solid material is not pure SiC but composition of SiC and some other material. It is possible to extract Debye model of

50PPI 10 mm thick material sample because it is homogeneous and isotropic compared to wavelength and for that reason absorption is dominant mechanism. For the other samples, scattering effects start to have influence on the measured parameters and materials' behavior cannot be described with Debye model. Also, extracted Deby model of 50PPI 10 mm sample cannot be applied to the other 50PPI samples of different thicknesses because of different densities of the samples and possible density gradient.

## 5. LOSS MECHANISMS IN SIC FOAM

In the previous paragraph we concluded that material used in our samples is conductive and lossy dielectric. Loss mechanisms in such materials are absorption, scattering and eddy currents. Which loss mechanism is dominant depends on the frequency of applied field and geometry and structure of the material. In the next subsections, with some approximations, we will estimate magnitudes of mentioned loss mechanisms. As a frequency dependent permittivity of material we will use extracted Debye permittivity model of 50PPI 10 mm sample (Eq. (3)). According to [14], permittivity of bulk material must have higher value than extracted effective permittivity of the foam sample.

### 5.1. Eddy Currents

The foam structure that we examined consists of pores that are surrounded by more or less circular rings. When the foam is exposed to varying electromagnetic field, and if our assumption is true that bulk material is conductive, then we have induction of electrical currents in the circular rings (by varying magnetic fields) which acts as additional losses. In that case even if material is non magnetic, because of eddy currents real part of the complex permeability is different than 1, while imaginary part is not equal 0. In the case of pure SiC, because it is low loss material at microwave frequencies, eddy currents do not exist. To estimate magnetic losses due to eddy currents we used simplified model: rings are circular, randomly distributed inside of material and there are no coupling effects between them. In order to have a feeling about magnitude of losses produced by eddy currents, as frequency dependent permittivity of material we used values given by Eq. (3). In this model permeability is given by Eq. (4). Detailed explanations and derivations are in [20].

$$\mu = \frac{1}{1 - i\frac{A}{3}} \tag{4}$$

$\mu$ is calculated permeability due to eddy currents, with:

$$A = \frac{W\varepsilon'' \left(\frac{\pi f a}{c}\right)^2}{1 - iX} \tag{5}$$

$$X = \frac{f\sigma LS}{a} \tag{6}$$

$W$ is volume fraction ocupied by rings; $\varepsilon''$ is imaginary part of materials permittivity; $c$ is speed of light; $f$ is frequency; $\sigma$ is conductivity of material related to imaginary part of permittivity; $L$ is ring inductance related to ring dimensions; $S$ is conductor cross section; $a$ is radius of conducting ring.

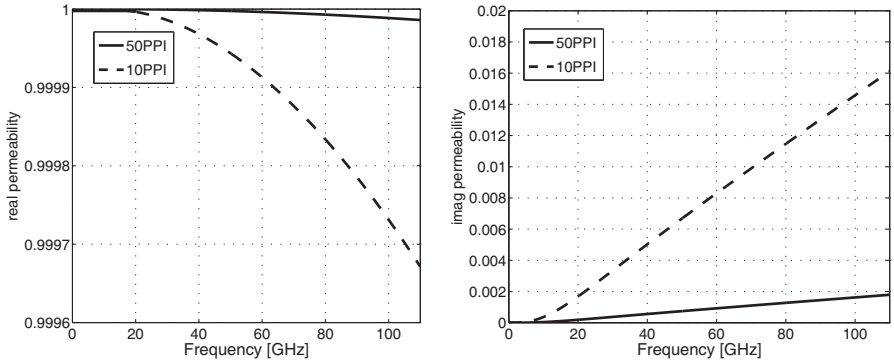


**Figure 10.** Estimated real and imaginary part of frequency dependent permeability due to eddy currents in 10PPI and 50PPI samples.

Figure 10 represents estimated permeability for 10PPI and 50PPI samples. We see that permeability of 50PPI sample is smaller than permeability of 10PPI sample. It is due to different ring radii (eddy currents depend more on the ring radius than on its cross section). Ring radius of 10PPI sample is approximately 1.5 mm, while for the 50PPI material it is approximately 0.6 mm. We can conclude that eddy currents effect is more visible in the foams with the bigger pore size and when material is lossy. Realistic situation of our material differs from simplified model. Conductive rings are randomly distributed (foam is isotropic along all three axes) but they are connected. Connections between rings have effects on the current distribution within the ring.

### 5.2. Absorption and Scattering

Absorption and scattering are loss mechanisms that occur simultaneously. Which one will be dominant depends on the chemical com-

position of the particles, their size, shape, surrounding material and on the other side on polarization state and frequency of the incident beam. Term 'extinction' includes both absorption and scattering. To approximately predict magnitude of absorption and scattering that happen in the foam, we calculate Mie efficiencies. Mie efficiencies are dimensionless numbers and efficiencies that we calculate are $Q_{ext}$ (extinction efficiency), $Q_{abs}$ (absorption efficiency) and $Q_{sca}$ (scattering efficiency) [12]. Equations from which we calculate Mie efficiencies are 7 to 11. Detailed equations as well as MATLAB code for Mie efficiencies calculations are in [13]. Because of the complex structure of the foam, we calculate efficiencies for the spherical particles which radius is approximate radius of the point where three or more ligaments connect and second calculation is for the sphere which radius is equal to the radius of the cross section of the ligament.

Mentioned dimensions are given in the Table 2 for both 10PPI and 50PPI foams. Another approximation is related to the material from which spheres are made. Since we do not have any information about bulk material from which our samples are made, in calculation of Mie efficiencies we use frequency dependent permittivity given by Eq. (3). Figures 11 and 12 represent Mie efficiencies for different sphere dimensions.

$$Q_{ext} = Q_{abs} + Q_{sca} \tag{7}$$

$$Q_{sca} = \frac{2}{x^2}\sum(2n+1)\left(|a_n|^2 + |b_n|^2\right) \tag{8}$$

$$Q_{ext} = \frac{2}{x^2}\sum(2n+1)Re(a_n + b_n) \tag{9}$$

$$a_n = \frac{m^2 j_n(mx)[xj_n(x)]' - j_n(x)[mxj_n(mx)]'}{m^2 j_n(mx)[xh_n^{(1)}(x)]' - h_n^{(1)}(x)[mxj_n(mx)]'} \tag{10}$$

$$b_n = \frac{j_n(mx)[xj_n(x)]' - j_n(x)[mxj_n(mx)]'}{j_n(mx)[xh_n^{(1)}(x)]' - h_n^{(1)}(x)[mxj_n(mx)]'} \tag{11}$$

$m$ is refractive index of the sphere; $x = \frac{2\pi a}{\lambda}$ is the size parameter depending on the ratio between the sphere radius a and wavelength; $a$ is radius of sphere; $j_n$ and $h_n$ are spherical Bessel functions; primes $'$ are the first derivatives with respect to the arguments.

**Table 2.** Parameters for Mie efficiencies calculation.

| Sample | Ligament radius [mm] | Sphere radius [mm] |
|---|---|---|
| 10PPI | 0.3 | 1.25 |
| 50PPI | 0.05 | 0.25 |

## 6. DISCUSSION ON MEASUREMENTS AND SIMULATIONS

### 6.1. 10PPI Samples

X band measurements show that for 17 mm and 28 mm thick samples $S_{11_m}$ is below $-10$ dB, while for 10 mm thick sample that is not the case. In X band there are different $S_{11_m}$ for different thicknesses because that is low frequency range compared to particle size ($\lambda$ is much bigger then the size of constituents of the foam cell). Measurements in K and Ka band are independent of the sample thickness and $S_{11_m}$ decrease with increasing frequency. Figure 11 shows that, for the given ligament cross section and used permittivity values, over whole frequency range absorbtion is dominant over scattering. In Figure 12 estimated Mie efficiencies for 10PPI material show dominance of absorption over scattering up to 60 GHz and the opposite for higher frequencies. Measurements done up to the end of Ka frequencies show monotonically decrease in $S_{11_m}$. Above approximately 60 GHz frequency, scattering is taking role over absorption and because of the complex materials' structure it is expected to have complex interference of the scattered waves. As additional losses, eddy currents can be considered. Imaginary part of permeability that comes from eddy currents increases up to frequency of 60 GHz and then slowly decreases.

### 6.2. 50PPI samples

In Figures 11 and 12 we see that for 50PPI samples absorption is dominant over scattering up to frequencies of 110 GHz. Influence

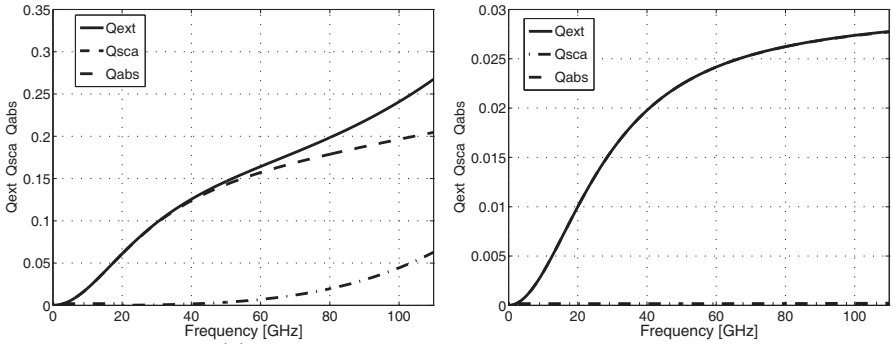


**Figure 11.** Calculated Mie efficiencies based on ligament cross section of 10PPI material (a) and 50PPI material (b).

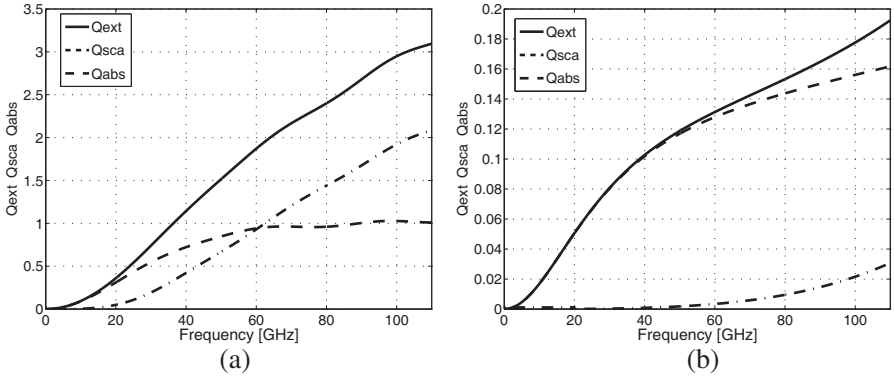


**Figure 12.** Calculated Mie efficiencies based on ligament joint point dimensions of 10PPI material (a) and 50PPI material (b).

of eddy currents is small (Figure 10) but increases with frequency. Ligament dimensions are small compared to wavelength of the incident electromagnetic field and 50PPI samples look homogeneous at examined frequencies. Transmission measurements of 10 mm thick sample are fitted with Debye model (Eq. (3)). Measurements in K and Ka band show thickness independent value of $S_{11_m}$ which lies between $-10$ dB and $-15$ dB.

## 7. CONCLUSION

Measured reflection results that we presented are comparable with other microwave radiation absorbers. In [21], it is presented that 3 cm thick multilayer composition of foamed material (foamed polymer/CNT nanocomposite) has $S_{11_m}$ in the range from 8 to 16 GHz lower than $-10$ dB. If we compare our measurements in the same frequency range, we see that with thinner samples, we achieve the same or lower reflection.

Our samples' volume fraction is 16 to 18 percents and independent on the pore size. That means bigger pore size has thicker ligaments and vice versa. From measurements as well as Mie efficiency simulations we can conclude that in examined frequency range 10PPI samples show better performances than 50PPI samples. Since they are with the similar volume fraction, if they are of the same thicknesses (and different pore size), they will have the same weight. That means in terms of weight there is no advantage of one sample pore size over the other.

## REFERENCES


1. Nornikman, H., et al., "Setup and results of pyramidal microwave absorbers using rice husks," *Progress In Electromagnetics Research*, Vol. 111, 141–161, 2011.
2. Wang, J., et al., "Three-dimensional metamaterial microwave absorbers composed of coplanar magnetic and electric resonators," *Progress In Electromagnetics Research Letters*, Vol. 7, 15–24, 2009.
3. Ramprecht, J., M. Norgren, and D. Sjoberg, "Scattering from a thin magnetic layer with a periodic lateral magnetization: Application to electromagnetic absorbers," *Progress In Electromagnetics Research*, Vol. 83, 199–224, 2008.
4. Harris, C. I., et al., "Progress towards SiC products," *Applied Surface Science*, No. 184, 393–398, 2001.
5. Siegel, P. H., R. H. Tufas, and P. Goy, "A simple millimeter wave blackbody load," *Ninth International Conference on Space THz Technology*, March 17–19, 1998.
6. Klaassen, T. O., et al., "Optical characterization of absorbing coatings for submillimeter radiation," *12th International Conference on Space THz Technology*, February 14–16, 2001.
7. Zhao, D. L., F. Luo, and W. C. Zhou, "Microwave absorbing property and complex permittivity of nano SiC particles doped with nitrogen," *Journal of Alloys and Compounds*, Vol. 490, 190–194, 2010.
8. Su, X., et al., "Improvement of permittivity of SiC with Al doping by combustion synthesis using $Al_2O_3$," *Journal of Alloys and Compounds*, Vol. 492, L16–L19, 2010.
9. Zhang, H., J. Zhang, and H. Zhang, "Numerical predictions for radar absorbing silicon carbide foams using a finite integration technique with a perfect boundary approximation," *Smart Materials and Structures*, Vol. 15, 759–766, 2006.
10. Zhang, H., J. Zhang, and H. Zhang, "Computation of radar absorbing silicon carbide foams and their silica matrix composites," *Computational Materials Science*, Vol. 38, 857–864, 2007.
11. Shvets, G., "Photonic approach to making a material with a negative index of refraction," *Phys. Rev. B*, Vol. 67, No. 3, 2003.
12. Bohren, C. F. and D. R. Hufman, *Absorption and Scattering of Light by Small Particles*, Wiley-VCH, Weinheim, 2004.
13. Mätzler, C., *MATLAB Functions for Mie Scattering and Absorption*, IAP Research Report, No. 2002-08, Institut für

Angewandte Physik, Universität Bern, 2002.

14. Sihvola, A., *Electromagnetic Mixing Formulas and Applications*, IEE Electromagnetic Waves Series 47, London, 1999.
15. Watari, K., et al., "Effect of grain boundaries on thermal conductivity of silicone carbide ceramic at 5 to 1300 K," *J. Am. Ceram. Soc.*, Vol. 86, No. 10, 1812–1814, 2003.
16. Takeuchi, Y., et al., "RF dielectric properties of SIC ceramics and their application to design of HOM absorbers," *Proceedings of the Particle Accelerator Conference*, 1195–1197, May 16–20, 2005.
17. Kaatze, U., "Techniques for measuring the microwave dielectric properties of materials," *Metrologia*, Vol. 47, No. 2, S91–S113, 2010.
18. Kumar, A. and G. Singh, "Measurement of dielectric constant and loss factor of the dielectric material at microwave frequencies," *Progress In Electromagnetics Research*, Vol. 69, 47–54, 2007.
19. Göllei, A., et al., "Apparatus and method to measure dielectric properties ($\varepsilon'$ and $\varepsilon''$) of ionic liquids," *Review of Scientific Instruments*, Vol. 80, No. 044703, American Institute of Physics, 2009.
20. Mätzler, C., "Eddy currents in heterogeneous mixtures," *Journal of Electromagnetic Waves and Applications*, Vol. 2, Nos. 5–6, 473–479, 1988.
21. Molenberg, I., et al.,"Foamed nanocomposites for EMI shielding applications," *Advanced Microwave and Millimeter Wave Technologies: Semiconductor Devices, Circuits and Systems*, Intech, March 2010.